A Study of the Effects of Mounting Supports, and Dissipation on a Piezoelectric Quartz Double-Ended Tuning Fork Gyroscope

Gobong Choi[1] and Yook-Kong Yong[2]

[1, 2]Dept. of Civil and Environmental Engineering, 623 Bowser Road, Rutgers University, Piscataway, NJ 08854, U.S.A.
[1]gobong.choi@rutgers.edu, [2]yyong@rci.rutgers.edu

Abstract: A COMSOL model of a piezoelectric quartz double ended tuning fork gyroscope was implemented. The gyroscope has two detection modes; the first mode detects the angular velocity about a z-axis perpendicular to the tuning fork plane (x-y plane), while the second mode detects the angular velocity about a y-axis that is the longitudinal axis along the length of the tuning fork. Eigenfrequency analyses with geometric parameters were performed to maximize the sensitivity of the gyroscope. Frequency response analyses were used to simulate the response of the gyroscope to angular velocity about its z-axis. The Coriolis forces were treated as body forces in the COMSOL model. The sign and magnitude of the change in charge at the detection electrodes are proportional to the sign and magnitude of the angular velocity of the gyroscope. A sensitivity analysis was performed for the detection of z-axis angular velocity as a function of the silicon rubber adhesive thickness. The adhesive height would affect the production yields of this gyroscope.

Keywords: Piezoelectric vibratory gyroscope, quartz, double ended tuning fork, two-axis gyroscope, dissipation, electrical parameters,

1. Introduction

The gyroscope is a device for measuring the changes in angular momentum, and it can detect angular velocity from the Coriolis force applied to the sensor. In this paper, we study the piezoelectric quartz double-ended tuning fork gyroscope [1] that is a type of vibratory gyroscope.

In general, vibratory gyroscopes have a main driving mode and one or more sensing modes. The vibratory gyroscopes use the Coriolis force to detect the angular momentum. When the gyroscope is given an angular velocity, the main driving mode is required to interact with the angular velocity to produce a harmonic Coriolis force that excites a sensing mode. The sensing mode in turn produces a change in charge or voltage at the sensing electrode. The vibratory tuning fork gyroscope faces substantial practical problems because its sensing modes are easily influenced by the mounting supports and lead installation of the sensing element.

The Coriolis force F_c is a fictitious force that only appears in a rotating non-inertial reference frame. It is given by the formula [2]:

$$\boldsymbol{F}_c = m * \boldsymbol{a}_c = 2 * m * \boldsymbol{\Omega} \times \boldsymbol{v} \qquad (1)$$

Where m is the proof mass, a_c is the Coriolis acceleration, Ω is the angular velocity vector of the rotating frame and v is the velocity vector of the mass in the reference frame. Due to the cross product of v and Ω in Eqn. (1), $\boldsymbol{F}_c = 0$ when the velocity vector $\boldsymbol{v}$ is parallel to the angular velocity vector $\boldsymbol{\Omega}$.

We further refer to [2] in which a simple theoretical model of a z-axis gyroscope was employed to explain the operating principles of a vibratory gyroscope. It was comprised of a proof mass m suspended in the x-y plane. Mass m can oscillate in two orthogonal directions as shown in Fig. 1. The driving direction was the x-direction and detecting direction was the y-direction. The external force drove the proof mass m at the resonance frequency in the driving (x-) direction. If the supporting frame was rotated with an angular velocity about the z-axis, a Coriolis force in the y-direction was generated and applied to the proof mass. The simplified two-degree of freedom (2-dof) equations of motion for this z-axis gyroscope are:

$$m\ddot{u} + C_x\dot{u} + k_x u = \tau_x \qquad (2)$$

$$m\ddot{v} + C_y\dot{v} + k_y v = \tau_y - 2m\Omega_z\dot{u} \qquad (3)$$

Where τ_x is the external harmonic excitation force in the driving direction, τ_y is the total external force in the detecting direction, and $2m\Omega_z\dot{u}$ is the Coriolis force induced by the cross product of the angular velocity Ω_z rotation about

the z-axis and momentum $m\dot{u}$ in the x-direction. If there were no angular velocity, the Coriolis force is zero.
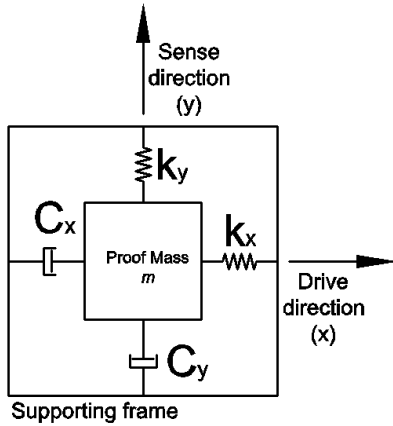

Figure 1: A simple theoretical model of a z-axis gyroscope.

2. Piezoelectric Quartz Double-Ended Tuning Fork Gyroscope

The quartz crystal is a very common material used in piezoelectric devices. It is stable, and has zero temperature coefficient cuts for various modes of vibrations. For a tuning fork, a popular cut is a rotated Z-cut quartz that exhibits a parabolic frequency-temperature curve. In this paper we study the piezoelectric quartz double-ended tuning fork gyroscope using a Z-cut quartz crystal blank.
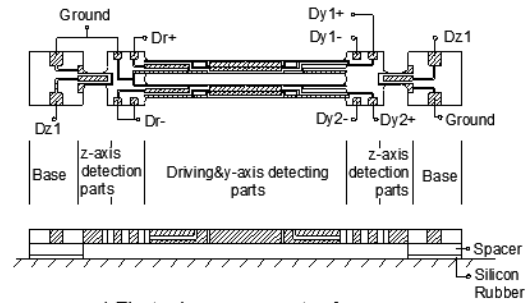
2.1 Structure of the double-ended tuning fork gyroscope.

The structure of the quartz double-ended tuning fork gyroscope is shown in Figure 2, along with its electrode configurations. This structure was obtained from references 1, 3, and 4. There are three main components of the gyroscope. The first main component is the mounting supports that include the quartz crystal spacers and silicon rubber adhesive that are located at each end of the gyroscope. The second component is the driving electrodes (Dr $\pm$) and y-axis detecting electrodes ((Dy $\pm$) that are located at the center arms of the gyroscope. The last component is the z-axis detecting electrodes ((Dz $\pm$) that are located between the mounting supports and the driving and y-axis detecting electrodes.

The electrodes are thin films made of gold. The thickness of the driving electrodes could be adjusted for fine tuning the driving mode

frequency by using the mass loading effect of the electrodes. The gyroscope was designed so that the moment and the displacement of the mounting support are minimized while the moment of the detecting arms was maximized.

The dimensions of the gyroscope are provided in Table 1 below.

a) Electrode arrangements of gyroscope
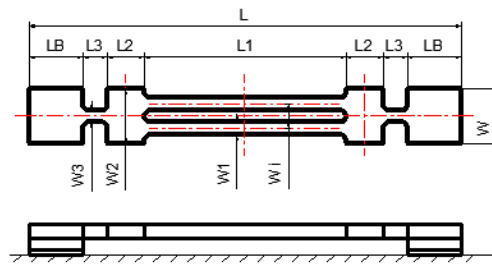
b) Dimension of the gyroscope

Figure 2: Structure of the double ended tuning fork gyroscope: (a) Electrode arrangements of gyroscope, (b) Dimensions of the gyroscope

2.2 Principles of operation of the double ended tuning fork gyroscope.

Figure 3 shows the three modes of vibrations that are employed by the gyroscope to detect angular velocities about the y- and z-axes of the device: (a) At the top is the driving mode which is a flexure mode in the x-y plane, (b) at the middle is the y-axis (Ωy) detection mode which is a flexure mode in the y-z plane, and (c) at the bottom is the z-axis (Ωz) detection mode which is a asymmetric flexure mode in the x-y plane.

The driving electrodes are designed to vibrate the center arms in the horizontal x-y plane as shown in Fig.3 (a). The top arms vibrate in the opposite x-direction from the bottom arm. The Coriolis force Fcy is generated in z-direction when an angular velocity Ωy is applied to the gyroscope. Due to the Coriolis Effect, the center

arms then vibrate in *y-z* plane as shown in Fig.3 (b). The *y*-axis detecting electrodes on the center arms of the gyroscope detect the Coriolis force *F*cy. For maximum detection sensitivity of angular velocity about the *y*-axis, the natural frequency of the *y*-axis detection mode must match closely the natural frequency of the driving mode.

(a) Driving Mode

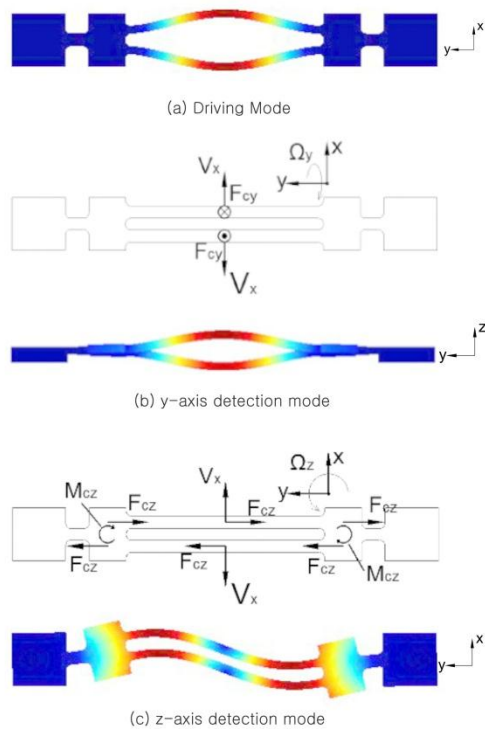(b) y-axis detection mode

(c) z-axis detection mode

Figure 3: The three modes of vibration of the gyroscope: (a) Driving mode, (b) y-axis detection mode and (c) z-axis detection mode.

The principle of operation of the *z*-axis detection mode is same as the *y*-axis detection mode except that the Coriolis force is generated in the *y*-direction. The driving arms are vibrating in the horizontal *x-y* plane as shown in Fig.3 (a). When the *z*-axis angular velocity *Ω*z is applied to the gyroscope, a pair of Coriolis forces *F*cz is produced as shown in Fig.3(c). The pair of Coriolis forces *F*cz act on the center arms in the opposite direction and generate a moment *M*cz at the base of the gyroscope as shown in Fig.3(c). The moment *M*cz generates the asymmetric mode in the horizontal *x-y* plane that in turn causes the arm L3 (see Fig. 2(b)) to bend. The *z*-axis detecting electrodes on the arm L3 detect

the Coriolis force *F*cz. For maximum detection sensitivity of angular velocity about the *z*-axis, the natural frequency of the *z*-axis detection mode must match closely the natural frequency of the driving mode.

3. COMSOL Multiphysics Modeling and Simulation

The COMSOL 4.2a was used to simulate the FEM model of the gyroscope. The 3-D Structural Mechanics, Piezoelectric Devices (pzd) module was employed to model the structure of the quartz gyroscope. The FEM model of the gyroscope is shown in Fig.4. Tetrahedral elements were used in the mesh. There were 50,594 elements and 321,757 degrees of freedom.
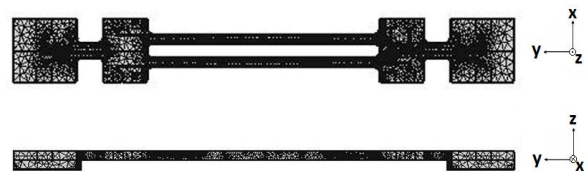

Figure 4: COMSOL Multiphysics FEM mesh of the double-ended tuning fork Z-cut quartz gyroscope.

Both eigenfrequency and frequency response analyses were performed. The eigenfrequency analysis was employed to (1) determine the optimum gyroscope geometry for the driving mode and two detection modes, and (2) to calculate the electrical parameters of the gyroscope. The frequency response analysis was needed to calculate the Coriolis forces and the detection sensitivity of the gyroscope.

3.1 Eigenfrequency analysis

Since the sensitivity of the gyroscope is dependent on the matching of the natural frequencies of the detecting modes to the natural frequency of the driving mode, parametric-eigenfrequency analyses were performed on the geometry of the tuning fork. The parameters were the height of the mounting supports and the thickness of the quartz blank. These parameters affect the frequencies of the driving mode and the detecting modes.

For example, Fig.5 shows the changes in the *y*-detection and *z*-detection mode frequencies and the driving mode frequency as a function of the thickness of the resonator-gyroscope when W3 = 0.491 mm. We observed that it is difficult to get all three modal frequencies to match, especially

the y-detection mode frequency. At the resonator thickness t = 0.36031 mm the three modes come closest together but there is coupling of the y-detection mode with the driving and z-detection modes. This coupling creates cross-talking of the y-detection mode with the z-detection mode. Hence in this paper we focused on a one axis detection gyroscope, namely, the z-axis angular velocity detection while putting aside for now the y-axis angular velocity detection.
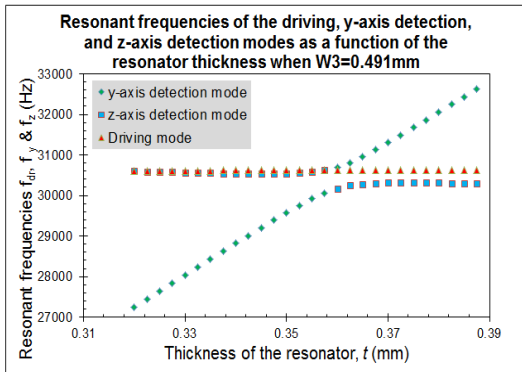

Figure 5: Resonant frequencies of the driving, y-axis detection, and z-axis detection modes as a function of the resonator thickness when W3 = 0.491 mm

It is possible to match very well the frequency of the z-detection mode to the frequency of the driving mode. Figure 6 shows that a good frequency match could be obtained at a resonator thickness of 0.3 mm.
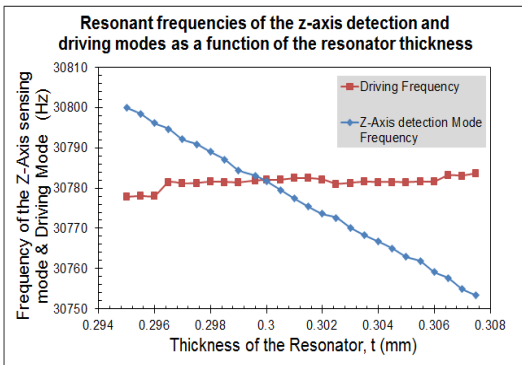

Figure 6: Resonant frequencies of the z-axis detection mode and the driving mode with the resonator thickness when W3 = 0.43 mm.

The normalized resonant frequency of the z-axis detection mode depends on the width W3. The width W3 is adequate at W3=0.491mm, as shown in figure 7. The change in the width W3

has very little effect on the driving and y-axis detection modes frequencies. We also observed that the resonant frequency of the z-axis detection mode can be tuned by the width W3.
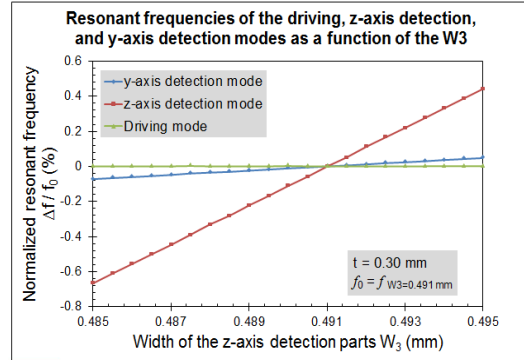

Figure7: Resonant frequencies of the driving, z-axis detection and y-axis detection modes as a function of the W3

We can further optimize the frequency matching of the z-detection mode. Figure 8 shows the change in frequency of the z-detection mode as a function of the spacer height. The blue line is for W3=0.491 mm while the red line is for W3=0.49 mm. (W3 is the width of the arm at the base (please see figure 2(b)).
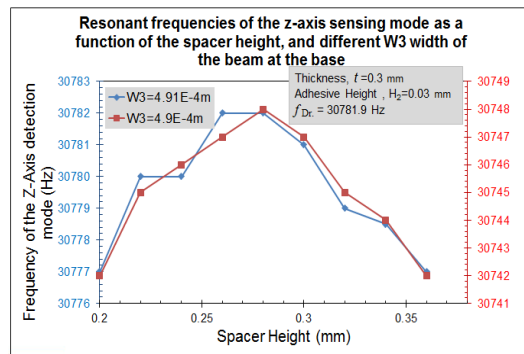

Figure 8: Change in resonant frequencies of the z-axis detection mode for height of the spacer.

Based upon our parametric studies, we chose the resonator dimensions to be those provided in the Table I below:

Table I: Dimensions of the double ended tuning fork gyroscope. (Please see Figure 2 (b) for the definition of the dimension)

(Unit: mm)

Item	Dimension	Item	Dimension
L	16.0	W	2.00
L1	7.46	W1	0.31
L2	1.38	W2	1.60
L3	0.89	W3	0.43
LB	2.00	Wi	0.75
t (blank thickness)	0.30	Spacer	0.28
Silicon rubber	0.03		

3.2 Butterworth van Dyke electrical parameters

The piezoelectric gyroscope could be represented in an equivalent circuit parameters of the Butterworth van Dyke resonator (Figure 9).
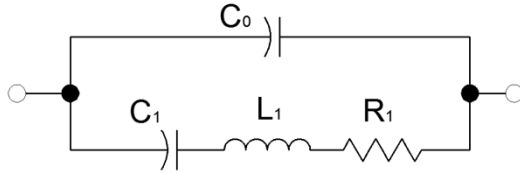

Figure 9: Equivalent electrical circuit parameters of the piezoelectric resonator-gyroscope represented as Butterworth van Dyke resonator.

The static capacitance C_0 is obtained from a COMSOL electrostatic analysis by putting 1 V on the drive electrodes. C_0 is then equal to the total surface charge on the drive electrodes (Eqn.4). The electrical parameters C_1, L_1, and R_1 can be obtained from our eigenfrequency analysis of the resonator-gyroscope. The following four quantities are first obtained from the eigenfrequency analysis:
(1) ω_r, the short circuit resonance frequency,
(2) Q, the quality factor of the mode ω_r,
(3) q, the charge on the drive electrode, and
(4) E, an energy norm.
Q and ω_r are obtained directly from the COMSOL eigenfrequency model $pzd.Q\_eig$ and $pzd.omega$, respectively, while q and E are calculated using Eqns. 4 and 5, respectively:

$$q = |\int_{drive\ electrode}(pzd.nD)dA| \quad (4)$$

$$E = \int_{all\ domains}(pzd.rho * pzd.disp\texttt{^}2)\,d\Omega \quad (5)$$

The four quantities ω_r, Q, q, and E are used to calculate the electrical parameters C_1, L_1, and R_1 using Eqns.6, 7 and 8 below:

$$C_1 = q^2/(E*\omega_r^2) \quad (6)$$

$$L_1 = 1/(C_1*\omega_r^2) \quad (7)$$

$$R_1 = 1/(Q*C_1*\omega_r) \quad (8)$$

The calculated Butterworth van Dyke electrical parameters for our gyroscope are provided in Table II below:

Table II. Calculated equivalent circuit elements

Frequency (Hz)	30781.69
C_1 (F)	1.0347E-15
R_1 (Ω)	3332.4965
L_1 (H)	25837.8089
C_0 (F)	1.83941E-10

3.3 Dissipation, quality factor Q, and motional resistance R_1

It is important that the dissipation or damping of the gyroscope be modeled because of its effect on the electrical parameters and sensitivity of the gyroscope. The quality factor Q obtained from the COMSOL model is dependent on the damping coefficients of the quartz elastic constants, and the dissipation in the silicon rubber adhesive used to bond the gyroscope to a device substrate. Eqn.8 shows that the motional resistance R_1 is inversely proportional to the Q if the motional capacitance C_1 is constant.

Since the model damping will affect the coupling between resonant modes, and the resonant frequencies of the modes themselves, the dissipation at the silicon rubber adhesive bonds was studied and found to be an important factor in the sensitivity of the gyroscope when subjected to an angular velocity about the z-axis. This is shown in section 3.5 below.

3.4 Frequency response analysis of the resonator-gyroscope

The sensitivity of the gyroscope to angular velocity about the z-axis was simulated with the frequency domain (harmonic response) analysis of COMSOL. The frequency response of the driving mode with 1 V at the drive electrodes is shown in Figure.10.
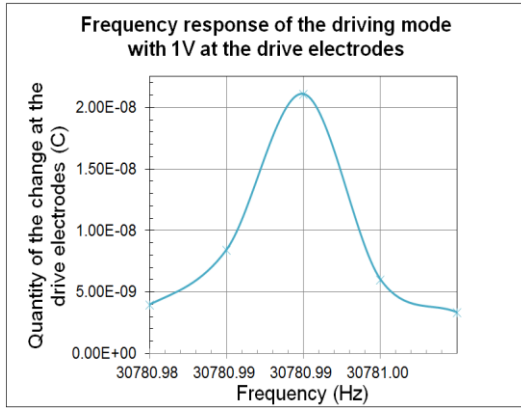
Figure 10: COMSOL frequency response of the driving mode with 1 V at the drive electrodes.
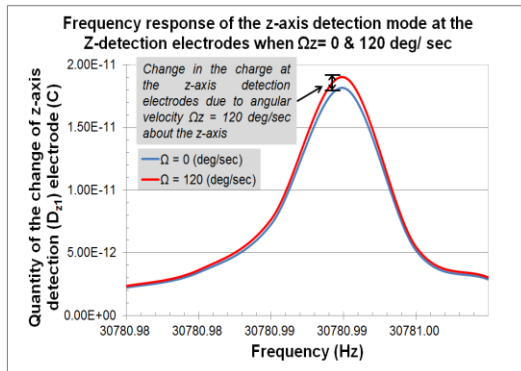

Figure 11: Change in charge at the z-axis detection electrodes when the gyroscope experiences an angular velocity $\Omega_z = 120$ deg. /s about its z-axis.

In order to study the sensitivity of the gyroscope to an angular velocity about the z-axis, we apply the following Coriolis-body forces on the entire structure of the COMSOL model of the gyroscope:

$$b_x = j2\rho\Omega_z\omega v \tag{9}$$

$$b_y = -j2\rho\Omega_z\omega u \tag{10}$$

$$b_z = 0 \tag{11}$$

Where b_x, b_y, and b_z are the body forces in the x-, y-, and z-directions, respectively. The displacements in the x- and y-direction are u and v respectively. Also j, ρ, Ω_z, and ω are respectively $\sqrt{-1}$, mass density of quartz, and angular velocity about the z- axis. We observe a change in the charge at the z-detection electrodes when the gyroscope is rotated about the z-axis. For example in a frequency response analysis

shown in Fig.11 we see the change in charge at the z-detection electrodes when $\Omega_z = 120$ deg. /s. Therefore the gyroscope could sense the angular velocity Ω_z about the z-axis as a change in charge at the z-axis detection electrodes. The magnitude of the change is greatest at the resonant frequency of the driving mode.

3.5 Sensitivity analysis of the gyroscope

The sensitivity of the gyroscope is dependent on the matching of the resonant frequency of the z-axis detection mode to the resonant frequency of the driving mode. When the two resonant frequencies are not well matched the sensitivity of the gyroscope decreases.

We studied the effect of small changes in the thickness of the silicon rubber adhesive at the bottom of the spacers of the gyroscope (please see Figure 2a). The adhesive thickness has significant effects on the z-axis detection mode frequency but has little or no effect on the driving mode frequency. The change in the z-axis detection mode frequency resonator will affect the sensitivity of gyroscope when subjected to an angular velocity about its z-axis. This is shown in Fig.12 where we observe that a small change of 4µm in adhesive thickness could change the sensitivity by as much as 44%. Therefore the adhesive thickness will be a significant factor in improving the production yields of this gyroscope.
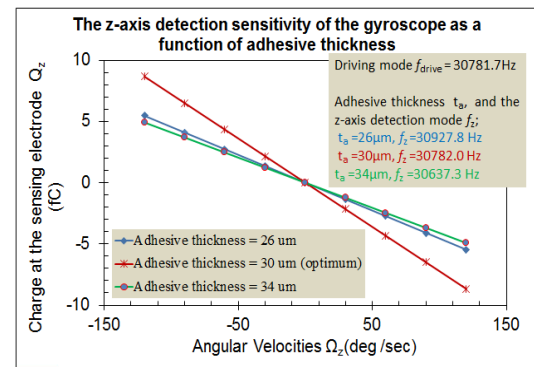

Figure 12. The z-axis detection sensitivity of the gyroscope as a function of adhesive thickness.

4. Summary and Conclusions

A COMSOL model of a piezoelectric quartz double ended tuning fork gyroscope was successfully implemented. The gyroscope has two detection modes; the first mode detects the angular velocity about a Z- axis perpendicular to

the tuning fork plane (X-Y plane), while the second mode detects the angular velocity about a Y-axis that is the longitudinal axis along the length of the tuning fork. The quartz double-ended tuning fork gyro sensor characteristics were studied using COMOL software.

Both eigenfrequency and frequency response analyses were performed. The eigenfrequency analysis was employed to (1) determine the optimum gyroscope geometry for the driving mode and two detection modes, and (2) to calculate the electrical parameters of the gyroscope. The frequency response analysis was needed to calculate the Coriolis forces and the detection sensitivity of the gyroscope.

An optimal geometry of the gyroscope was found by eigenfrequency analyses with geometric parameters such as the dimensions of the tuning fork tines, spacers, and resonator thickness. The dimensions of the gyroscope provided in Table I were obtained using eigenfrequency analyses.

The frequency response analysis was used to simulate the response of the gyroscope to angular velocity about its z-axis. The Coriolis forces were treated as body forces in the COMSOL model which cause change in charge at the detection electrodes. The sign and magnitude of the change in charge at the detection electrodes are proportional to the sign and magnitude of the angular velocity of the gyroscope. We observed that good frequency matching of the driving mode with the detection modes was essential for the gyroscope to function well as a sensor for angular velocity.

A sensitivity analysis was performed for detection of z-axis angular velocity as a function of the silicon rubber adhesive thickness at the bottom of the spacers. The z-axis detection mode was found to be sensitive to the adhesive height. Conversely the driving mode was found to be insensitive to the adhesive height. Therefore the adhesive height is an important factor in the matching of the z-detection mode frequency to the driving mode frequency. The adhesive height would affect the production yields of this gyroscope.

5. References

1. K. Sato, A.Ono, and Y. Tomikawa, Experimental Study of Gyro Sensor Using Double Ended Tuning Fork Quartz Resonator, Jpn. J. Appl. Phys, Volume 43, pp.3000-3003 (2004)
2. C.Acar and A.Shkel, MEMS Vibratory Gyroscope: Structural Approaches to Improve Robustness, pp18-23. Springer-Verlag New York Inc., New York, NY (2008)
3. K. Sato, A.Ono, and Y. Tomikawa, Simulation of quartz gyro-sensor using double-ended tuning fork resonator for detection of two-axial angular velocity, IEEE Ultrasonics Symposium, pp.1350-1353(2003)
4. K. Sato, A.Ono, and Y. Tomikawa, Finite element method simulation of double-ended tuning-fork quartz resonator for application to vibratory gyro-sensor, Jpn. J. Appl. Phys, Volume 42, pp.3115-3119 (2003)